Masters of Science, Applied Mathematics

Numerical Analysis of Deconvolution Closure for Mesoscopic Continuum Models of Particle Systems

Eric Nathan Johnson
Washington State University
Department of Mathematics
enjohnson@math.wsu.edu

Advisor: Dr. Kevin Cooper
Graduate Committee Members:
Dr. Alexander Panchenko
Dr. Sergey Lapin

March 28, 2014

Abstract

We examine a method of solving a microscale continuum model for a microscale particle system using mesoscale integral approximations. Previously an attempt was made to solve the nonlinear equations numerically, but the results were unstable. To follow up on those results, we attempt to linearize and solve the integral system numerically using Runge-Kutta methods. The linear approximation will serve as a predictor. Then a nonlinear corrector will be used to modify the linear solution. These results will be compared against cluster output of the exact microscale solutions.

Contents

List of Figures

1 Introduction

We are interested in solving for the location of particles in time in a d-dimensional particle system over some short period of time T. We have $N \gg 1$ identical particles P_i on some computational domain $\Omega \in \mathbb{R}^d$. The total mass of the system is denoted M. Each particle i has some velocity $\mathbf{v}_i$ and position $\mathbf{q}_i$ and is influenced by both inter-particle and external forces.

To satisfy physical law the system of particles must satisfy a system of ordinary differential equations [1]

$$\dot{\mathbf{q}}_i = \frac{d\mathbf{q}_i}{dt} = v_i, \tag{1}$$

$$\frac{M}{N}\dot{\mathbf{v}}_i = \mathbf{f}_i + \mathbf{f}_i^{(ext)}, \tag{2}$$

subject to initial conditions,

$$\mathbf{q}_i(0) = \mathbf{x}_i, \tag{3}$$
$$\mathbf{v}_i(0) = \mathbf{v}_i^0, \tag{4}$$

where

(i) $\mathbf{f}_i^{(ext)}$ denotes external forces (gravity, confining forces)

(ii) $\mathbf{f}_i$ are pair interparticle forces

$$\mathbf{f}_i = \sum_j \mathbf{f}_{ij}.$$

We wish to study asymptotic behavior as $N \to \infty$. Scaling is required to bound the amount of energy in the system independent of N. An example of this scaling is:

$$\begin{aligned}\mathbf{f}_{ij} &= -\frac{1}{N}\nabla_{\mathbf{q}_i} U\left(\frac{|\mathbf{q}_i - \mathbf{q}_j|}{\varepsilon}\right), \\ &= -\frac{1}{\varepsilon N}\frac{d}{d\xi}U(\xi),\end{aligned}$$

where forces are generated by a finite range pair potential $U(\xi)$ where ξ is the distance away from a particle.

Instead of solving these ordinary differential equations directly on the microscale, we will use integral approximations for the required properties on the mesoscale. We replace the exact microscopic quantities with regularized deconvolution approximations.

To find the averages, we define a windowing function, ψ, that satisfies

$$\int \psi(\mathbf{x})d\mathbf{x} = 1.$$

To convert to the mesoscale we scale with η,

$$\psi_\eta(\mathbf{x}) = \eta^{-d}\psi\left(\frac{\mathbf{x}}{\eta}\right).$$

This window function will allow us to generate averages of micro-scale dynamical functions.

The mesoscopic *average density* is:

$$\bar{\rho}^\eta(t,\mathbf{x}) = \frac{M}{N}\sum_{i=1}^{N}\psi_\eta(\mathbf{x}-\mathbf{q}_i(t)). \tag{5}$$

And the mesoscopic *average momentum* is:

$$\bar{\rho}^\eta\bar{v}^\eta(t,\mathbf{x}) = \frac{M}{N}\sum_{i=1}^{N}\mathbf{v}_i(t)\psi_\eta(\mathbf{x}-\mathbf{q}_i(t)). \tag{6}$$

Consider $\psi = (c_d)^{-1}\chi(x)$, where χ is the characteristic function of the unit ball in $\mathbb{R}^d$ and c_d is the volume of the unit ball. Then

$$\bar{\rho}^\eta = \frac{1}{c_d\eta^d}\frac{M}{N}\sum\chi\left(\frac{\mathbf{x}-\mathbf{q}_i(t)}{\eta}\right).$$

The right hand size gives the number of particles located within distance η of x at time t. M/N is the mass of individual particles.

Differentiating (5) and (6) with respect to t and using (1) and (2) yields *exact mesoscopic balance equations* for the primary variables:

$$\begin{aligned}
\frac{\partial}{\partial t}\bar{\rho}^\eta(t,\mathbf{x}) &= \frac{d}{dt}\frac{M}{N}\sum\psi_\eta(\mathbf{x}-\mathbf{q}_i(t)) \\
&= -\frac{M}{N}\sum\frac{\partial\psi_\eta}{\partial t}(\mathbf{x}-\mathbf{q}_i(t))\ \mathbf{q}_i'(t) \\
&= -\frac{M}{N}\sum\frac{\partial\psi_\eta}{\partial t}(\mathbf{x}-\mathbf{q}_i(t))\ \mathbf{v}_i(t),
\end{aligned}$$

$$\begin{aligned}
\frac{\partial}{\partial t}\bar{\rho}^\eta\bar{\mathbf{v}}^\eta(t,\mathbf{x}) &= \frac{d}{dt}\frac{M}{N}\sum\mathbf{v}_i(t)\psi_\eta(\mathbf{x}-\mathbf{q}_i(t)) \\
&= \frac{M}{N}\left(\mathbf{v}_i'(t)\psi_\eta(\mathbf{x}-\mathbf{q}_i(t)) + \mathbf{v}_i(t)\frac{\partial\psi_\eta}{\partial t}(\mathbf{x}-\mathbf{q}_i(t))\mathbf{q}_i'(t)\right) \\
&= \frac{M}{N}\left(\mathbf{v}_i'(t)\psi_\eta(\mathbf{x}-\mathbf{q}_i(t)) + \mathbf{v}_i^2(t)\frac{\partial\psi_\eta}{\partial t}(\mathbf{x}-\mathbf{q}_i(t))\right).
\end{aligned}$$

Conservation of mass and momentum balance equations take the form:

$$\partial_t\bar{\rho}^\eta + \mathrm{div}(\bar{\rho}^\eta\bar{\mathbf{v}}^\eta) = 0, \tag{7}$$

$$\partial_t(\bar{\rho}^\eta\bar{\mathbf{v}}^\eta) + \mathrm{div}(\bar{\rho}^\eta\bar{\mathbf{v}}^\eta\otimes\bar{\mathbf{v}}^\eta) - \mathrm{div}\mathbf{T}^\eta = 0. \tag{8}$$

The *convective stress* is

$$\mathbf{T}^{\eta}_{(c)}(t,\mathbf{x}) = -\sum m_i(\mathbf{v}_i - \bar{\mathbf{v}}^{\eta}(t,\mathbf{x})) \otimes (\mathbf{v}_i - \bar{\mathbf{v}}_i{}^{\eta}(\mathbf{x},t))\psi(\mathbf{x}-\mathbf{q}_i),$$

and the *interaction stress* is taken over all pairs (i,j) of particles that interact with one another

$$\mathbf{T}^{\eta}(t,\mathbf{x})_{(int)} = \sum_{(i,j)} \mathbf{f}_{ij} \otimes (\mathbf{q}_j - \mathbf{q}_i) \int_0^1 \psi_{\eta}(s(\mathbf{x}-\mathbf{q}_j) + (1-s)(\mathbf{x}-\mathbf{q}_i))ds.$$

The total stress is then $\mathbf{T}^{\eta} = \mathbf{T}^{\eta}_{(c)} + \mathbf{T}^{\eta}_{int}$.

2 Numerical Approximations

2.1 Process Overview

The mesoscale partial differential equations (7), (8) provide a way of approximating the solution to the discrete microscale problem (1), (2). However, a previous attempt at solving the nonlinear mesoscale problem numerically was unstable.

To make progress, we sought to understand the nonlinear system better. To this end, Dr. Panchenko linearized the mesoscale problem. Efforts were made to understand related linear systems and to investigate different Runge-Kutta schemes for solving these systems. We then implemented several numerical schemes to test the methods. It was found that the numerical methods used were not responsible for the instability.

We then went back to the nonlinear problem with the intention of using the linearization to produce a numerical predictor. This would allow us to advance a solution quickly and stably in time. Then a nonlinear corrector would be developed to keep the numerical solution closer to the exact microscale solution. To produce a nonlinear corrector, the convective and interaction stress integrals were solved numerically.

We will restrict ourselves to a 1-dimensional system. The numerical predictor-corrector scheme will be compared against an associated microscale problem run on a cluster.

2.2 Interpolated Problem

Introduce suitable interpolating functions $\tilde{v}$ for velocity and $\tilde{q}$ for position for a uniform grid $\{x_j\}$ that satisfy

$$\begin{aligned} \tilde{q}(0, x_j) &= q_j^0 \\ \tilde{v}(0, \tilde{q}(0, x_j)) &= v_j^0 \end{aligned}$$

initially, and

$$\begin{aligned} \tilde{q}(t, x_j) &= q_j(t) \\ \tilde{v}(t, \tilde{q}(t, x_j)) &= v_j(t) \end{aligned}$$

at other times.

In a one-dimensional case the mesoscopic balance equations become

$$T_{(c)}^{\eta}(t,x) = -\frac{M}{L}\int_0^L (\tilde{v}(t,y) - \bar{v}^{\eta}(t,x))^2 \psi_{\eta}(x-y) J(t,y)\, dy, \tag{9}$$

which is *convective stress*. The *interaction stress* is

$$T_{(int)}^{\eta}(t,x) = -\frac{N-1}{N}\int_0^L U'\left(\frac{L}{J(t,y)}\right)\int_0^1 \psi_{\eta}\left(x - y - \frac{sh}{J(t,y)}\right)\, ds\, dy. \tag{10}$$

The *conservation of mass* and *momentum* equations are then

$$\partial_t \bar{\rho}^\eta + \partial_x(\bar{\rho}^\eta \bar{v}^\eta) = 0 \tag{11}$$

$$\partial_t(\bar{\rho}^\eta \bar{v}^\eta) + \partial_x(\bar{\rho}^\eta(\bar{v}^\eta)^2) - \partial_x(\bar{T}^\eta_{(c)} + \bar{T}^\eta_{(int)}) = 0. \tag{12}$$

2.3 Linearization

In [2], Dr. Panchenko linearized (11) and (12) system to obtain

$$\partial_t \tilde{\rho} + \rho_0 \partial_x \tilde{v} = 0, \tag{13}$$

$$\rho_0 \partial_t \tilde{v} - \partial_x \tilde{T}_{(int)} = 0, \tag{14}$$

where

$$\tilde{T}_{int} = -\frac{L^2}{M}\tilde{\rho} \cdot A$$

and

$$A = \sum_{p=1}^{p_*} p^2 U''(Lp).$$

Here $M > 0$ denotes the mass, $L > 0$ is the width of the interval occupied by the particles. where p_* denotes the total number of particles affected. U is some potential function. Typically p_* is 2 or 3.

Making these substitutions we find that

$$\rho_0 \partial_t \tilde{v} + \frac{L^2 A}{M}\partial_x \tilde{\rho} = 0.$$

Eliminating $\tilde{\rho}$ gives the *wave equation* in terms of $\tilde{v}$

$$\partial_{tt}\tilde{v} - \frac{L^2 A}{M}\partial_{xx}\tilde{v} = 0. \tag{15}$$

2.4 Predictor

2.4.1 Wave Equation

Let $c^2 = L^2 A/M$, and we have a standard wave equation that describes velocity of the interpolation $\tilde{v}$ on a closed interval $x \in [0, L]$

$$\partial_{tt}\tilde{v} - c^2 \partial_{xx}\tilde{v} = 0, \tag{16}$$

with initial conditions and periodic boundary conditions

$$\tilde{v}(x, 0) = f(x) = 1,$$
$$\tilde{v}_t(x, 0) = g(x) = v_0.$$

A solution via separation of variables will give us an analytic result to compare our numerical method against. The general solution to the wave equation is

$$\tilde{v}(x,t) = \sum_{n=1}^{N} [A_n \cos(\lambda_n t) + B_n \sin(\lambda_n t)] \sin(\frac{n\pi}{\ell} x)] + \sum_{n=1}^{N} [C_n \cos(\lambda_n t) + D_n \sin(\lambda_n t)] \cos(\frac{n\pi}{\ell} x)].$$

The constants A_n, B_n, C_n and D_n depend upon f, g, the initial conditions and boundary conditions. This approximated analytic solution was plotted against Runge-Kutta numerical solutions to test the viability of using Runge-Kutta methods to solve the wave equation.

2.4.2 Runge-Kutta and Strong Stability Preserving Runge-Kutta

We will discretize the spatial component of (16) to put it into a matrix form Au for Runge-Kutta methods. Let $x_0 = 0$ and $x_N = L$. Define $h = x_i - x_{i-1}$ as a uniform spacing of the partition and a uniform time step as $k = t_i - t_{i-1}$. Let $\mathbf{u} = (u(x_0,t), u(x_1,t), ..., u(x_N,t))^T$ where each x_i is an element of a uniformly spaced partition $x_0 < x_1 < \ldots < x_N$. Then we obtain a $O(h^2)$ discretized system of first order equations.

$$u_{xx}(x,t) \approx \frac{u_{h+1}^k - 2u_h^k + u_{h-1}^k}{h^2}$$

From this we obtain a matrix A that operates on $\mathbf{u}$ that discretizes the wave equation into the form $\mathbf{u}_{tt} = A\mathbf{u}$.

For the left side, we make the following substitution

$$\mathbf{v} = \mathbf{u}_t$$
$$\mathbf{v}_t = \mathbf{u}_{tt},$$

and let

$$\mathbf{U} = \begin{bmatrix} \mathbf{u} \\ \mathbf{v} \end{bmatrix}.$$

Then the discretization may be written as a matrix equation

$$\mathbf{U}_t = \begin{bmatrix} \mathbf{u} \\ \mathbf{v} \end{bmatrix}_t = \begin{bmatrix} \mathbf{v} \\ A\mathbf{u} \end{bmatrix} = \begin{bmatrix} 0 & I \\ A & 0 \end{bmatrix} \begin{bmatrix} \mathbf{u} \\ \mathbf{v} \end{bmatrix} \tag{17}$$

which is suitable for a Runge-Kutta scheme.

Call the block matrix $\mathbf{A}$. We will use SSPRK(3,3) as defined in [4]. This is an optimal third-order method:

$$\mathbf{U}^{(1)} = \mathbf{U}^n + \triangle t \mathbf{A}(\mathbf{U}^n)$$
$$\mathbf{U}^{(2)} = \frac{3}{4}\mathbf{U}^n + \frac{1}{4}\mathbf{U}^{(1)} + \frac{1}{4} \triangle t \mathbf{A}(\mathbf{U}^{(1)})$$
$$\mathbf{U}^{n+1} = \frac{1}{3}\mathbf{U}^n + \frac{2}{3}\mathbf{U}^{(2)} + \frac{2}{3} \triangle t \mathbf{A}(\mathbf{U}^{(2)}).$$

SSP Runge-Kutta methods are suitable for solving systems of ordinary differential equations in the form

$$U_t = -f(U)_x,$$

which arise commonly in problems involving hyperbolic conservation laws. The spatial derivative is discretized to obtain $L(U)$ using finite differences or finite elements. $L(U)$ has the property that for some sufficiently small time step $\triangle t \leq \triangle t_{FE}$, which must satisfy the Courant-Friedrichs-Levy (CFL) condition, and first-order Euler time discretization

$$U^{n+1} = U^n + \triangle t L(U^n),$$

the total variation of the one-dimensional discrete solution does not increase in time. This ensures that the method maintains a strong stability property

$$TV(U^{n+1}) \leq TV(U^n) \text{ for } TV(U^n) := \sum_j |U^n_{j+1} - U^n_j|,$$

while achieving high order accuracy in time [7].
For comparison we also used a standard fourth-order Runge-Kutta (RK4):

$$\begin{aligned}
\mathbf{U}^{(1)} &= \mathbf{A}\mathbf{U}^n \\
\mathbf{U}^{(2)} &= \mathbf{A}\left(\mathbf{U}^n + \frac{\triangle t}{2}\mathbf{U}^{(1)}\right) \\
\mathbf{U}^{(3)} &= \mathbf{A}\left(\mathbf{U}^n + \frac{\triangle t}{2}\mathbf{U}^{(2)}\right) \\
\mathbf{U}^{(4)} &= \mathbf{A}\left(\mathbf{U}^n + \triangle t\mathbf{U}^{(3)}\right) \\
\mathbf{U}^{n+1} &= \mathbf{U}^n + \frac{\triangle t}{6}\left(\mathbf{U}^{(1)} + 2\mathbf{U}^{(2)} + 2\mathbf{U}^{(3)} + \mathbf{U}^{(4)}\right).
\end{aligned}$$

These schemes were used to approximate solutions to (13) and (14) to form a predictive time step for the nonlinear problem.

We can think of the initial state of the system as an $n \times 1$ vector containing all ones for each x_i, which is $\mathbf{U}^0$:

$$\mathbf{U}^0 = u(x, 0) = [\mathbb{1}]$$

In each case, the vector values of $\mathbf{U}_t$ were found numerically using Matlab.

Both Runge-Kutta implementations were very close to the analytic solution found using separation of variables. The infinity norm of the difference between SSPRK and RK4 implementations were calculated to be within 4×10^{-9}. For this reason, Runge-Kutta order 4 was used for all subsequent calculations.

2.5 Corrector

From [1], we have the integral approximations of stresses for the microscale problem.

From equation (9), we have an integral approximation for the *convective stress*:

$$T^{\eta}_{(c)}(t,x) = -\frac{M}{L}\int_0^L (\tilde{v}(t,y) - \bar{v}^{\eta}(t,x))^2 \psi_{\eta}(x-y) J(t,y)\ dy,$$

where $\tilde{v}(t,y)$ is the interpolation of the velocity, $\bar{v}^{\eta}(t,x)$ is the average velocity on the mesoscale, $\psi_{\eta}(x-y)$ is the windowing function and $J(t,y)$ is the Jacobian.

From equation (10): we have an integral approximation for the *interaction stress*:

$$T^{\eta}_{(int)}(t,x) = -\frac{N-1}{N}\int_0^L U'\left(\frac{L}{J(t,y)}\right)\int_0^1 \psi_{\eta}\left(x - y - \frac{sh}{J(t,y)}\right)\ ds\ dy$$

where U' is the derivative of a potential function. In this case we use the Lennard-Jones potential U:

$$U(\xi) = 4\epsilon\left[\left(\frac{\sigma}{\xi}\right)^{12} - \left(\frac{\sigma}{\xi}\right)^{6}\right]$$
$$U'(\xi) = 24\epsilon\left[\left(\frac{\sigma^6}{\xi^7}\right) - \left(\frac{2\sigma^{12}}{\xi^{13}}\right)\right]$$

We may define $\epsilon = 0.25$ as the depth of the potential well, and let $\sigma = 2^{-1/6}$, which is the finite distance at which the potential is zero. ξ is the distance between particles.

We will approximate each using a midpoint approximation

$$\int_a^b f(y)\ dy \approx (\triangle y)\sum_{i=0}^{n-1} f(y_i)$$

where $(\triangle y) = \frac{b-a}{n}$ and $y_i = a + (i + \frac{1}{2})(\triangle y)$.

In order to evaluate these integrals we need to make the following substitutions.

$$\triangle y = \frac{b-a}{n} = \frac{L}{n},$$
$$y_i = \frac{iL}{n},$$
$$J(y_i) = \bar{\rho}^{\eta}.$$

$T^{\eta}_{(c)}(t,x)$, written independently of t, is

$$\begin{aligned} T^{\eta}_{(c)}(t,x) &= -\frac{M}{L}\int_0^L (\tilde{v}(y)-\bar{v}^{\eta}(x))^2\psi_{\eta}(x-y)J(y)\ dy \\ &\approx -(\triangle y)\frac{M}{L}\sum_{i=0}^{n-1}(\tilde{v}(y_i)-\bar{v}^{\eta}(x))^2\psi_{\eta}(x-y_i)J(y_i) \\ &\approx -\frac{\bar{\rho}^{\eta}M}{\eta n}\sum_{i=0}^{n-1}(\tilde{v}\left(\frac{iL}{n}\right)-\bar{v}^{\eta}(x))^2\psi\left(\frac{1}{\eta}\left(x-\frac{iL}{n}\right)\right). \end{aligned}$$

Meanwhile, $T^{\eta}_{(int)}(t,x)$ is a set of two nested integrals.

$$T^{\eta}_{(int)}(t,x) = -\frac{N-1}{N}\int_0^L U'\left(\frac{L}{J(t,y)}\right)\int_0^1 \psi_{\eta}\left(x-y-\frac{sh}{J(t,y)}\right)\ ds\ dy$$

However, the inner integral can be approximated simply:

$$\begin{aligned} \int_0^1 \psi_{\eta}\left(x-y-\frac{sh}{J(t,y)}\right)\ ds\ &\approx \frac{h}{2}\left[\psi_{\eta}\left(x-y-\frac{sh}{J(t,y)}\right)+\psi_{\eta}\left(x-y\right)\right] \\ &\approx \frac{L}{2\eta N}\left[\psi\left(\frac{1}{\eta}\left(x-y-\frac{L}{N\bar{\rho}^{\eta}}\right)\right)+\psi\left(\frac{1}{\eta}\left(x-y\right)\right)\right] \end{aligned}$$

Note that this is *inside* the outer integral variable dy, and so the interior stress can be evaluated as follows:

$$\begin{aligned} T^{\eta}_{(int)}(t,x) &\approx -\frac{N-1}{N}\int_0^L U'\left(\frac{L}{J(t,y)}\right)\int_0^1 \psi_{\eta}\left(x-y-\frac{sh}{J(t,y)}\right)\ ds\ dy \\ &\approx -\frac{N-1}{2N}\int_0^L U'\left(\frac{L}{J(t,y)}\right)\left[\psi_{\eta}(x-y)+\psi_{\eta}\left(x-y\frac{sh}{J(t,y)}\right)\right]\ dy \\ &\approx -\left(\frac{N-1}{2N}\right)\left(\frac{L^2}{2\eta N^2}\right)U'\left(\frac{L}{\bar{\rho}^{\eta}}\right)\sum_{i=0}^{n-1}\left[\psi\left(\frac{1}{\eta}\left(x-\frac{iL}{n}-\frac{L}{N\bar{\rho}^{\eta}}\right)\right)+\psi\left(\frac{1}{\eta}\left(x-\frac{iL}{n}\right)\right)\right] \end{aligned}$$

Both of these integrals were evaluated in Matlab. We hope to improve upon the linear approximation to the problem by using the integral balance equations to produce a nonlinear corrector. To this end, Dr. Cooper wrote a corrector as detailed in [3]. A reliable corrector is still in progress. However, a first version has been implemented. Results of this implementation follow.

3 Results

We compared both RK4 and SSPRK(3,3) with an approximate solution to the wave equation of arbitrary precision as detailed in section 2.4.1. Figure 1 shows SSPRK(3,3) in red '+' and RK4 in blue 'x'. On the left subplot the analytic solution is plotted as a black solid line.

Figure 1: Wave Equation and Runge-Kutta at 5 time steps

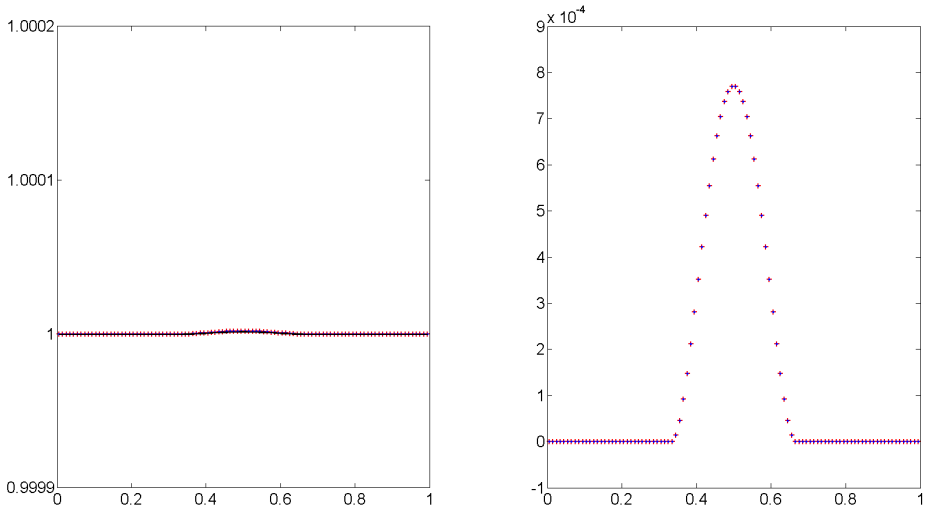

Both Runge-Kutta methods performed similarly well and the ℓ_2 norm of their difference was approximately 3×10^{-10} after 50 time steps. However, the ℓ_2 norm of the analytic solution and Runge-Kutta methods increased quickly in time. This was approximately 3×10^{-5} after 50 time steps. Figure 2 shows SSPRK(3,3) and RK4 again after 50 time steps.

Figure 2: Wave Equation and Runge-Kutta at 50 time steps

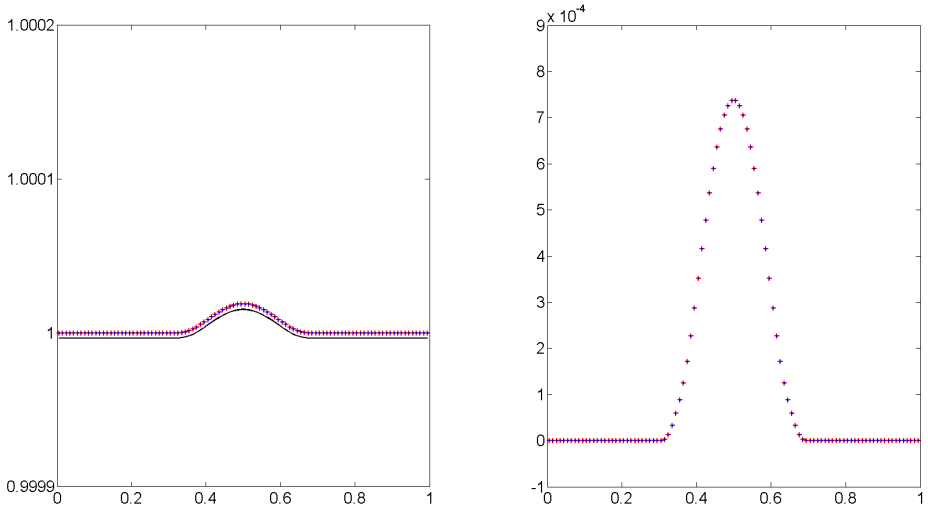

After 300 time steps the ℓ_2 norm of the difference between the two Runge-Kutta methods was

less than 2×10^{-9}. The ℓ_2 norm for the difference between the analytic solution and RK4 was about 2×10^{-4}.

Figure 3: Wave Equation and Runge-Kutta at 300 time steps

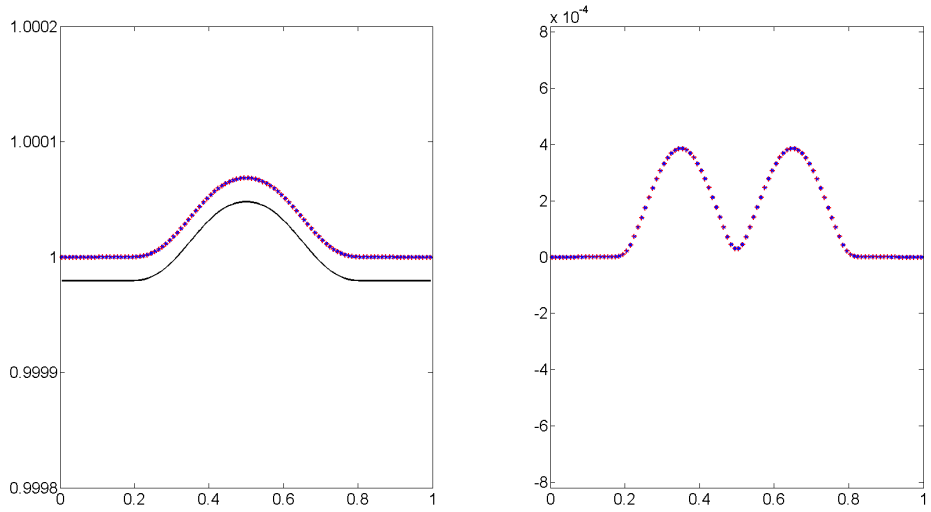

A time step of 0.005 with the domain $[0, 1]$ approximated with 100 subintervals was used to produce these figures.

The first version of a predictor-corrector scheme was implemented. In figures 4 - 7 the left subplot shows mesoscale verses microscale velocities. The right subplots are mesoscale verses microscale densities. The microscale data is from a cluster that is solving (1) and (2) with the Lennard-Jones potential.

Figure 4: Predictor-Corrector Initial State

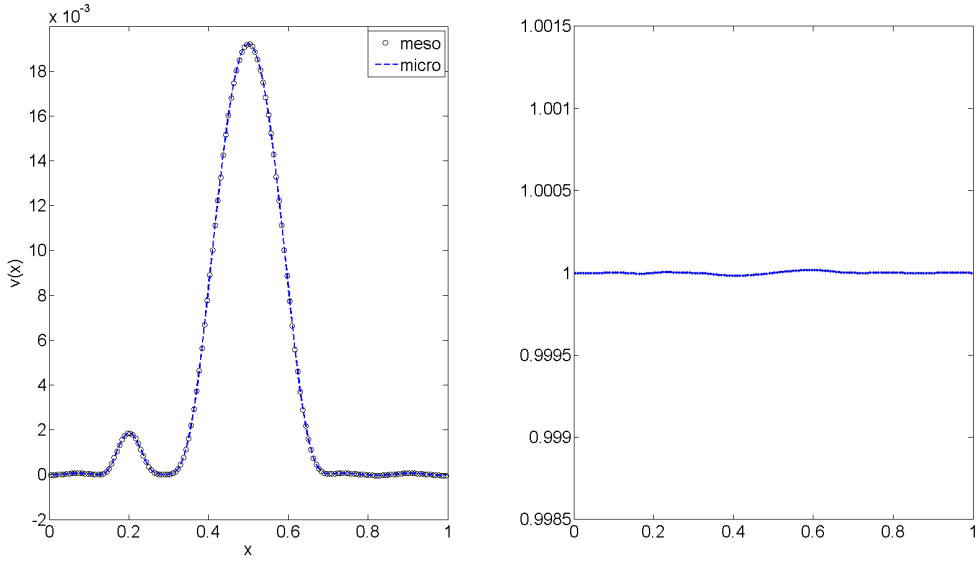

Figure 5: Predictor-Corrector after 25 iterations

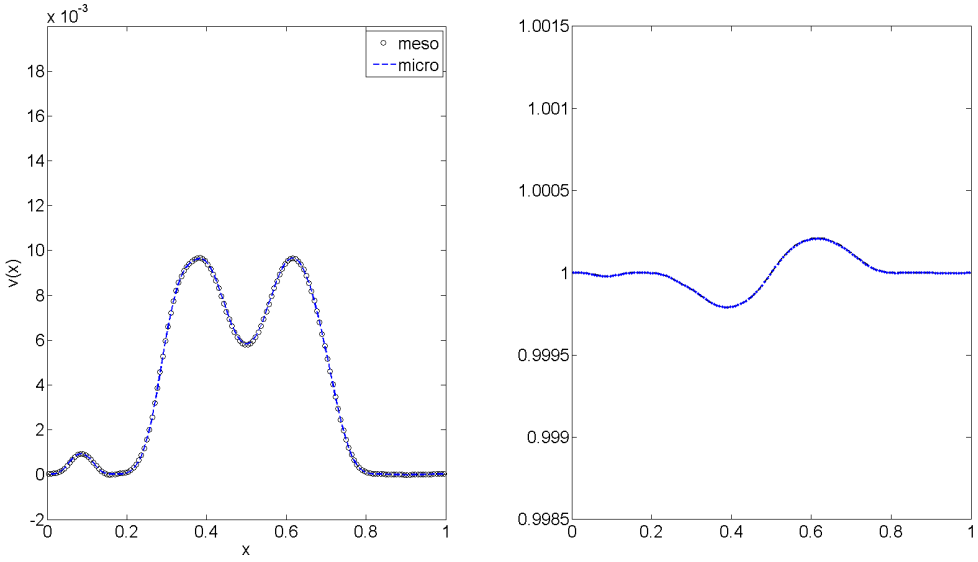

Figure 6: Predictor-Corrector after 50 iterations

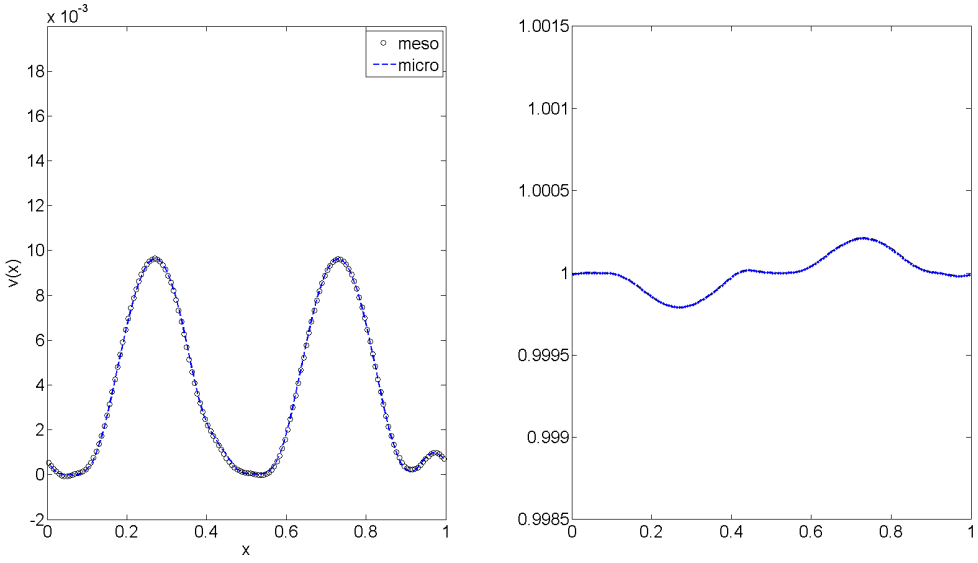

Figure 7: Predictor-Corrector after 75 iterations

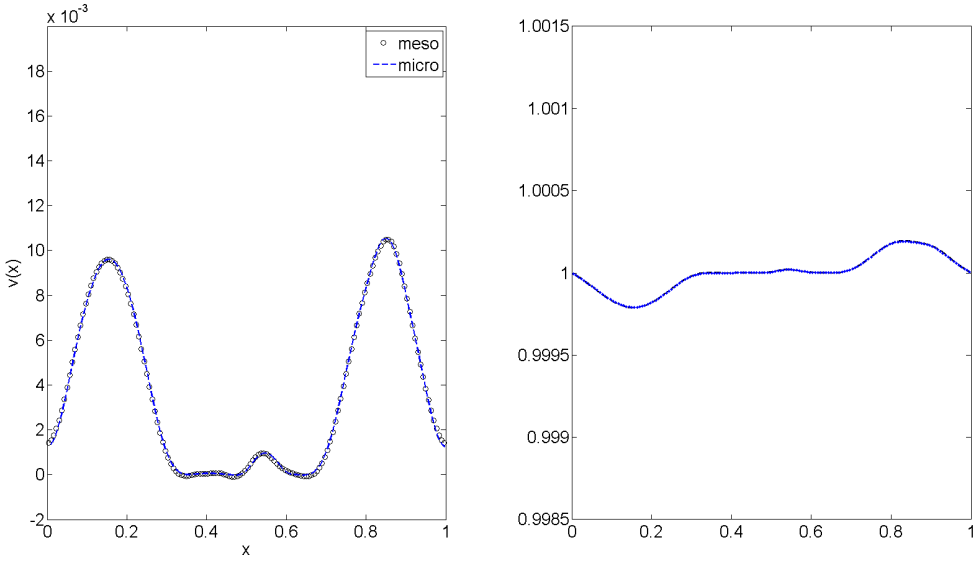

Each figure was produced using Matlab and the following parameters. The time step was 5×10^{-6} from $t = 0$ to $t = 0.01$. The parameters $\sigma = 0.06$, and $\epsilon = 0.1$ were chosen for the Lennard-Jones potential. From [6], we have a number 1.7652 that served as a constant in the velocity calculations.

4 Conclusions

The nonlinear nature of the mesoscale problem made solving the mesoscale system directly difficult. However, the linearization itself provides a good approximation to the microscale problem. The predictor-corrector method shows promise as a way of approximating the microscale problem. It is stable in time when a direct approach to solving the nonlinear mesoscale system was not. However the corrector itself does not provide a large improvement at this stage. Several attempts have been made to improve the corrector, but work remains to be done.

5 Bibliography

References

[1] Alexander Panchenko, Lyudmyla L. Barannyk, and Kevin Cooper, *Deconvolution Closure For Mesoscopic Continuum Models of Particle Systems*.

[2] Alexander Panchenko, *Linearization*. Unpublished note, 2013

[3] Kevin Cooper, *A proposed corrector for the wave equation applied to a 1-D particle system*. Unpublished note, 2014.

[4] Sigal Gottlieb, David I. Ketcheson, Chi-Wang Shu, *High Order Strong Stability Preserving Time Discretizations*. Jan 1, 2008.

[5] Sigal Gottlieb, *On High Order Strong Stability Preserving Runge-Kutta and Multi Step Time Discretizations*. Journal of Scientific Computing, Vol. 25, Nos. 1/2, November 2005.

[6] Kevin Cooper, *Lennard-Jones*. Unpublished note, March 2014.

[7] Sigal Gottlieb, David I. Ketcheson, Chi-Wang Shu, *Strong Stability-Preserving High-Order Time Discretization Methods*. Siam Review, Vol. 43, No. 1, February 2001.